Geomagnetic paleosecular variation recorded in Plio-Pleistocene volcanic rocks from Possession Island (Crozet Archipelago, southern Indian Ocean)

Pierre Camps, Bernard Henry, Michel Prevot, Liliane Faynot

Geomagnetic paleosecular variation recorded in Plio-Pleistocene volcanic rocks from Possession Island (Crozet Archipelago, southern Indian Ocean)

Pierre Camps*, Bernard Henry†, Michel Prévot* , and Liliane Faynot*

Abstract

Possession Island, in the Crozet Archipelago, consists of volcanic units erupted mainly between $\sim$ 5 and 0.5 Ma. A paleomagnetic sampling was carried out along several sections distributed near the northern, eastern, and southeastern coasts. A total of 45 independent flows were sampled (320 samples). For each flow a precisely defined characteristic remanence direction was usually isolated after a careful progressive cleaning in alternating fields. However, particularly complex remanence behavior is often observed. The magnetostratigraphy of the lava pile is quite simple, with reversed rocks in the lower part and normal units in the upper part of two sections. A third section is of normal polarity throughout its whole thickness, including three excursional directions. We did not find any intermediate directions between the normal and reverse magnetozones. Thus we have no evidence for the recording of the Matuyama-Brunhes transition expected from a previous study [1]. The amplitude of paleosecular variation, estimated from between-flow dispersion from the field of an axial dipole, is $11.8°$ with 95% confidence limits between $9.3°$ and $14.0°$. This value is consistent with the general anisotropic statistical model for paleosecular variation of *Constable and Johnson* [2].

1   Introduction

The existence of broad fluctuations in direction and magnitude, spanning a variety of spatial and temporal scales, is a fundamental characteristic of the Earth's magnetic field. These oscillations provide essential inputs for a better understanding of the field-generating process occurring in the Earth's outer core and they may also provide information on possible lateral changes at the core-mantle boundary. Yet there are still many uncertainties in the morphological characteristics of these fluctuations, as illustrated by many controversial debates. For example, the question of whether or not the transitional virtual

*Laboratoire Géophysique, Tectonique et Sédimentologie, CNRS and ISTEEM, Université Montpellier 2, Montpellier, France

†Laboratoire Géomagnétisme et Paléomagnétisme, CNRS and IPGP, Paris, France

geomagnetic poles (VGP) are preferentially confined to two sectors of opposed longitude, or the question of differences in paleosecular variation between the Pacific and Atlantic hemispheres, and moreover, if there are differences in paleosecular variation between the Northern and Southern Hemispheres as it is the case in the modern geomagnetic field (for a review, see [3]). These questions will undoubtedly remain unanswered as long as paleomagnetic analyses do not allow the development of reliable observations, both in terms of direction and intensity, from sites geographically dispersed. It is important to assess a good geographical coverage, preferably provided by volcanic rocks which are, in general, a more reliable recorder than sedimentary rocks.

In examining directional databases of volcanic records, McElhinny and McFadden [4] note a predominance of data acquired during an era before the modern methods of principal component analysis were introduced into the procedures for demagnetization of rocks. Therefore it is feared that some of these data are sullied with errors due to the presence of secondary components of magnetization which have not been completely eliminated. For this reason, McElhinny and McFadden [4] suggested that some of these studies would be worth repeating using modern experimental techniques. At first glance, this remark is particularly relevant to the volcanic data coming from the southern Indian Ocean, since they were obtained mainly at the beginning of the 1970s [1, 5, 6, 7, 8]. These data now appear crucial because they come from geographically isolated islands and thus represent rare field observations possible in a wide area devoid of data.

Spurred on by these considerations, we carried out a new paleomagnetic study of the volcanic sequences from Possession Island (Crozet Archipelago, southern Indian Ocean). This work was made possible by the presence of the French scientific base Alfred Faure on Possession Island, which enabled us to have essential logistical support for the paleomagnetic sampling. We also hoped to be able to sample the full spectrum of the field fluctuations, since a reversed to normal polarity boundary thought to correspond to Matuyama-Brunhes was detected and because some intermediate directions have been previously reported on this island [1].

2   Geological Setting

The Crozet Archipelago is composed of five main islands including Possession Island. This archipelago lies east of the Southwest Indian Ridge on an oceanic plateau which was created at 54 Ma during an episode of anomalous volcanism on the flank of the ridge, probably linked to a slow spreading phase [9]. Island volcanic edifices are being formed as this oceanic plateau passed over the Crozet hotspot. Detailed geological works [10, 11] indicate that Possession Island corresponds to a stratovolcano built through three main cycles, including five volcanic phases (Figure 1). The first cycle of activity, which likely lasted more than 7 Myr, constitutes the basement of a large stratovolcano of ~ 40 km diameter. Basaltic flows were first emplaced underwater (phase I) and later as subaerial or intrusive units (phase II). No age could be obtained from the very altered basalts from phase I. For the subaerial phase II flows, potassium-argon (K-Ar) ages of 8.1 ± 0.6 Ma and 2.7 ± 0.8 Ma were obtained [11] near the middle and the top of the sequence, respectively, whereas an age of 1.3 ± 0.4 Ma was

2

measured on a dyke. These ages correspond to several chrons preceding the Matuyama chron.

After a period of erosion the second cycle lasted for ~ 0.5 Myr. Conglomerate and differentiated felsic basalts of phase III lie, often unconformably, over the phase II formations. Phase III includes lava with K-Ar ages between 1.03 ± 0.4 and 0.72 ± 0.11 Ma (Matuyama-Lower Brunhes). The thick top plateau flows, assigned to phase IV, were erupted during volcanic activity along a wide rift oriented along a NW-SE azimuth of 135°. They yield radiometric ages from 0.70 ± 0.15 to 0.53 ± 0.09 Ma (Brunhes). Following a glacial episode during which U-shaped valleys were formed, the third cycle (phase V) produced recent Strombolian cones and some sparse lava flows (differentiated suite from felsic basalts to phonolites). This phase seems related to an important tectonic event marked by the formation of horsts and rifts and the collapse of a large western part of the stratovolcano.

3   Paleomagnetic Sampling

For paleomagnetic sampling, we looked for stratigraphic sections not affected by tectonic events and presumed to encompass a large time interval. One of *Watkins et al.'s* [1] paleomagnetic sections near the southeastern coast at Crique de Noël (CN), and a new one along the northern coast in the Petit Caporal valley (PC) (Figure 1) were chosen because they include volcanic sequences of flows from phases II and III and because one K-Ar age is available from each of them. Unfortunately, owing to very difficult field working conditions, we had to stop sampling before reaching the top of the PC section, leaving the upper part of the phase III sequence unsampled. A third section, with good quality outcrops, is located near the eastern coast on Alouette Mountain (AL). This volcanic sequence is exclusively composed of phase II lava flows. Because these three sections are several kilometers apart, a stratigraphic correlation from one section to the other was impossible independent of that provided by the magnetic data. It is noteworthy that we could not resample either *Watkins et al.'s* [1] section near Port Alfred, which is now in a protected area for sea birds, or his Morne Rouge section where no good outcrops were found. Instead, we tried to sample one section down from the Alfred Faure base at Bollard (BO) but could only collect cores from a single flow belonging to phase II. Along each section, we collected an average of seven cores from each consecutive volcanic unit using a gasoline-powered portable drill. Samples were oriented using a magnetic compass corrected for local anomaly by sighting the Sun and known landmarks. In all, we collected 320 oriented cores from 45 units. Flows are usually thin and seldom exceed 10 m in thickness. Because they are horizontal or near horizontal, no tilt correction has been made.

4   Experimental Procedure

Determination of the direction of characteristic remanent magnetization (ChRM) in the laboratory encountered several difficulties. First, the 15-day magnetic viscosity index [12, 13] was estimated on two thirds of the collection by measuring the remanent magnetization first after 2 weeks of storage with the ambient field

parallel to the positive cylindrical axis of each specimen ($\mathbf{M}_1$), and then after another two-week storage in zero field ($\mathbf{M}_2$). The viscosity index (ν) is expressed in percent by

$$\nu = \frac{|\mathbf{M}_1 - \mathbf{M}_2|}{|\mathbf{M}_2|}$$

with

$$\begin{aligned} \mathbf{M}_1 &= \mathbf{NRM} + \mathbf{VRM}_{Lab} \\ \mathbf{M}_2 &= \mathbf{NRM} \end{aligned}$$

where $\mathbf{NRM}$ is the "stable" natural remanent magnetization, which of course includes some viscous remanent magnetization (VRM) fraction acquired prior to the viscosity test, and $\mathbf{VRM}_{Lab}$ the VRM acquired during the first 2-week storage in the ambient field, and normally destroyed during the 2-week storage in zero field. Viscosity index measured from the Possession basalts ranges from <1% to >100%. It shows a lognormal distribution characterized by a median value of 5% and a geometric average of $15 \pm 3\%$ (95% interval for the mean) which is rather high compared to the mean value of $6.1 \pm 0.7\%$ found for some upper Tertiary and pre-Bruhnes quaternary subaerial volcanic rocks [13]. The high viscous index could be due to the presence in Possession basalts of nearly superparamagnetic single-domain grains as it has been shown for subaerial lava [13] or for synthetic magnetite [14]. The large number of highly viscous samples warns us that significant VRM overprints are likely, since the ratio of VRM acquired in situ since the beginning of the Bruhnes polarity epoch, to the ChRM is estimated for subaerial lava to be $\sim$ 3-4 times as large as the viscosity index [13]. Because we believe, as has been shown by one of us [13], that heating in a zero field is the most efficient cleaning method for VRM, we treated one pilot sample from each rock unit by stepwise thermal demagnetization using a noninductive PYROX furnace with a residual field <20 nT. Surprisingly, this treatment provided demagnetization diagrams of poor quality which were difficult to interpret (Figure 2c). This behavior, somewhat unusual for young basalts, could be explained by large instability of samples upon heating which is always observed for the few low-field susceptibility measurements performed under vacuum ($< 10^{-2}$ mbar) (Figure 3). Consequently, we decided to use alternating fields (AF) cleaning using a laboratory built AF demagnetizer in which the sample is stationary and subjected to fields up to 140 mT.

Second, during AF processing, many samples revealed an atypical easiness to acquire a spurious anhysteritic remanent magnetization (ARM) due to the presence of a small direct field in our device not previously detected. Thus we repeated, for these samples, each demagnetization step for two reversed positions of the sample then averaged the two measurements for each duplicated step in order to reduce the ARM effect on the calculated direction of the remaining NRM.

Finally, in a few cases for which the demagnetization curve does not decay to the origin (Figure 2e), we suspect that an artificial gyroremanent magnetization (GRM) was induced during AF cleaning. In principle, GRM is acquired by particularly anisotropic single domain grains [15, 16], in a direction perpendicular to both the applied AF axis and the easy axis of magnetization [17]. The GRM magnitude is maximum when the angle between AF and anisotropy axis is 45° and zero when these two axes are parallel or perpendicular to each other.

Therefore GRM is suppressed by demagnetizing and measuring successively each component at each step of the AF processing [18]. This measurement procedure greatly increased the quality of our demagnetization diagrams (Figure 2f). The overall complex remanence behavior prevented us from using the remanence intensities as proxy for paleointensity as was done with Icelandic and Hawaiian volcanic sequences [19]. Nor could we determine the absolute intensity of the paleofield, since very few samples satisfied the usual selection criteria.

5   Results

Following carefully chosen (to avoid spurious remanence) and very detailed AF demagnetization procedures involving up to 18 cleaning steps, the ChRM was successfully isolated from significant secondary components (Figure 4) for almost 90% of samples. We think that the natural magnetic overprint is likely of viscous origin because the components with low unblocking fields are generally directed along the present-day field direction. Thus we observe that the geometric average intensity of NRM is larger for the normal (6.2 ± 0.4 A/m, 95% interval confidence for the average) than for the reversely (2.2 ± 0.3 A/m) magnetized rocks. This interpretation is further validated by the rather large viscosity indices reported above. We determined the ChRM by means of a least-squares method [20]. Nearly all directions computed provide a maximum angular deviation of $< 2°$. Among the 10% of rejected samples are also those which gave a significantly different direction from that of the other samples from the same flow if field notes indicated possible misorientation. The flow average directions are listed together in Table 1 with the parameters from the Fisher's statistics. Only for flow PC7, no mean stable direction could be successfully determined. With the exception of flow PC1, the ChRM directions are well clustered in each flow with rather small values of the 95% confidence cone about the mean direction (α_{95}), all $<10°$.

We recommend that our results do not complete but supersede the ones described by Watkins et al. [1] because the directions do not corroborate each other, at least for the CN section which was resampled exactly at the same place, and because the former directions were calculated using the method of the minimum scatter criterion. This method, no longer used in current research, consisted of AF-demagnetizing specimens at various steps (maximum 30 mT in this case) and then combining the core directions obtained at any demagnetization steps to calculate the average direction yielding the minimum within-flow scatter. First, it is obvious that such a method is not suitable for rocks overprinted by large secondary components, as for many of the Possession Island basalts; a processing of 30 mT may not be sufficient to retrieve the primary component (Figure 5). Second, this method is not efficient in detecting the acquisition of spurious ARM and GRM components from AF treatment as low as 10 mT, as occurs in the present study. For example, we believe that the intermediate directions initially described by Watkins et al. [1] correspond to reversed directions which would have been incompletely cleaned of their present-day field viscous overprint. The principal component analysis used in the present study provides more reliable estimates of the paleofield directions.

6 Discussion

It seems very speculative to correlate one section to the others from the paleo-magnetic results. The main reason is that the magnetic sequences obtained are very simple, and thus they are not constraining in term of magnetostratigraphy. For sections PC and CN, reversed polarity units are found in the lower part and normal units are found in the upper part. Section AL is of normal polarity throughout its whole thickness, except for three consecutive flows yielding excursional directions. A notable result is the absence of intermediate directions between the normal and reverse magnetozones. We have, however, some arguments to suggest that the sampled sections do not duplicate each other and that altogether they cover a time interval long enough for providing a reliable record of the history of field fluctuations at Possession Island (Figure 6). The phase III units from the CN and PC sections are of normal polarity and therefore should have erupted during the Brunhes epoch, consistent with the K-Ar age of 0.72 Ma obtained in this sequence [11]. For the phase II basalts the reversed polarity obtained in the PC section in the top flows with K-Ar age of 2.7 ± 0.8 Ma [11] could correspond to the end of the Gilbert epoch or to the beginning of the Matuyama one. Then the bottom part of PC section, being also only of reversed polarity, should have been erupted during the same epoch. We have no clues for assigning a precise magnetic chron to the normal polarity zone corresponding to the whole section AL. We are certain, however, that flows belonging to the same chron have not been sampled elsewhere since phase II units from the other sections are of reverse polarity. The only doubt we have concerns the phase II units from BO section and the lower part of CN section. Because they are, like the phase II PC section, of reversed polarity, we assumed tentatively that they also belong to the beginning of Matuyama or to the end of Gilbert chron. Notwithstanding age uncertainties, it is likely that the three sections complement each other with no (or small) overlapping in time (Figure 6). Nevertheless, given the episodic nature of volcanism, the question remains whether the time elapsed between successive lava flows is long enough compared to the rate of secular variation of the geomagnetic field. If not, oversampling of the same field directions from lava flows clustered temporally will skew the estimate of the paleosecular variation. Unfortunately, without very accurate age determinations for each flow, we have no objective means of averaging or discarding similar successive directions, since the rate of secular variation is itself variable, and thus similar paleomagnetic directions may be due to real stasis of secular variation [21]. Thus we have to assume, tentatively, that the paleodirections obtained correspond to a reasonable random sampling of the field fluctuations over the Plio-Pleistocene period.

The characterization of the paleosecular variation was done by means of statistical techniques common in paleomagnetism. We processed the data by reversing the directions of reversed polarity and removing those having a VGP latitude less than an arbitrarily chosen cutoff to avoid inclusion of transitional data. The secular variation was estimated by the total angular standard deviation (asd) expressed in degrees as S_T in

$$S_T = (N-1)^{-\frac{1}{2}} \left(\sum_{i=1}^{N} \delta_i^2 \right)^{\frac{1}{2}},$$

where N is the number of data and δ_i is the angular distance between the *ith* field direction or VGP position and the direction or VGP position about which the dispersion is computed, corrected for the experimental errors by calculating the between-flow asd expressed in degrees as S_B in

$$S_B^2 = S_T^2 - S_W^2/\bar{n},$$

where $\bar{n}$ is the mean number of sample cores per lava, $S_W \approx 81°/\sqrt{\bar{\kappa}}$, and $\bar{\kappa}$ the mean precision parameter. The dispersion statistics of local field directions and corresponding VGPs are given in Tables 2 and 3, respectively, for two VGP cutoffs (45° and 55°), with analyses about means and an axial dipole. We stress that in the present study, the way the dispersion is estimated is not critical because first the mean direction is not statistically different from the direction of an axial dipole (Table 2) and second because the effect of experimental errors (the mean within-flow dispersion S_W) is rather small.

The present results agree better with the general anisotropic paleosecular model (CJ98.nz) proposed by Constable and Johnson [2] rather than with their model with axial anisotropy (CJ98). The preferred model CJ98.nz is able to generate complex geographical variations assuming that the boundary conditions at the core-mantle interface are geographically heterogeneous. The simulated asd values for VGPs (16.5°) and for directions (12°) for the Possession Island location are very close to the experimental ones found in the present study ($S_T = 16.8°$ and $s_B = 11.8°$, respectively). However, the experimental 95% confidence limits on asd (Tables 2 and 3), computed by means of the jackknife method [22], are rather wide and thus prevent a firm conclusion. To obtain a result with narrow confidence limits, we combined our data with those already published for Marion Island [7] which is located only 15° of longitude west to Crozet Archipelago. We did not include in this analysis the directions described from East Island [1], which is located 18 km east to the Possession Island because first East Island lava have similar petrological characteristics [23] than Possession basalts, and second the direction were obtained using the method of the minimum scatter criterion. Their reliability is thus questionable. The regional values of asd obtained (Table 3) are roughly the same as those obtained for Possession Island alone and thus still agree with the general anisotropic model CJ98.nz [2]. In the absence of intensity data we are not able to check more precisely this model, nor the Camps and Prévot's [19] model of fluctuations of the geomagnetic field.

The geomagnetic field excursion (N-T-N) recorded in the phase II lava from AL section is of particular interest (Figure 7) because it provides VGPs lying within one of the two preferred longitudinal bands for transitional VGPs obtained from sedimentary records [24]. This observation fits with the general anisotropic model, as do our PSV results. Still, the controversial question remains [25, 26] whether these preferred longitude sectors might be an artifact of remanence acquisition in sedimentary rocks [27] or indirect evidence for a thermal control of the Earth's core dynamics by the lower mantle [24].

7 Conclusion

We presented here a new paleomagnetic study of the volcanic sequence from Possession Island. This study emphasized the particularly complex behavior

of the remanence, which obliged us to apply particularly careful experimental procedures to isolate the ChRM. We think that such behaviors can explain our difficulties to corroborate the paleofield directions obtained in the present study and those previously reported [1], at least for the Crique de Noël section which was resampled exactly at the same place. In particular, we do not confirm the presence of intermediate directions within the Brunhes epoch. Hence we suggest that our directional results supersede the ones from the former study guessed to be less reliable. This raises the question of the reliability of the directions described from East Island (Crozet Archipelago), [1], since they have similar petrological and radiochronological characteristics [23]. Our paleosecular variation estimates seem to support models with longitudinal anisotropy. However, we do not have a sufficient number of paleofield directions to enable us to confirm this interpretation. For that, it would be necessary to repeat and complete a paleomagnetic study of lava flows from East Island in order to increase the number of paleomagnetic observations for this area of the Indian Ocean.

8   acknowledgments

References

[1] N.D. Watkins, A. Hajash, and C.E. Abranson. Geomagnetic secular variation during the brunhes epoch in the indian and atlantic ocean regions. *Geophys. J. R. astron. Soc.*, 28:1–25, 1972.

[2] C.G. Constable and C.L. Johnson. Anisotropic paleosecular variation models: Implications for geomagnetic field observables. *Phys. Earth Planet. Int.*, 115:35–51, 1999.

[3] R.T. Merrill, M.W. McElhinny, and P.L. McFadden. *The magnetic field of the Earth: Paleomagnetism, the core, and the deep mantle.* Academic press, San Diego, 1996.

[4] M.W. McElhinny and P.L. McFadden. Palaeosecular variation over the past 5 myr based on a new generalized database. *Geophys. J. Int.*, 131(2):240–252, 1997.

[5] N.D. Watkins and J. Nougier. Excursions and secular variations of the brunhes epoch geomagnetic field in the indian ocean region. *J. Geophys. Res.*, 78(26):6060–6068, 1973.

[6] N.D. Watkins, B.M. Gunn, J. Nougier, and A.K. Baksi. Kerguelen continental fragment or oceanic island? *Bull. Geol. Soc. Am.*, 85:201–212, 1974.

[7] C. Amerigian, N. Watkins, and B.B. Ellwood. Brunhes epoch geomagnetic secular variation on marion island: Contribution to evidence for a long-term regional geomagnetic secular variation maximum. *J. Geomagn. Geoelectr.*, 26:429–441, 1974.

[8] N.D. Watkins, I. McDougall, and J. Nougier. Paleomagnetism and potassium-argon age of st. paul island, south eastern indian ocean: contrasts in geomagnetic secular variation during the brunhes epoch. *Earth Planet. Sci. Lett.*, 24:377–384, 1975.

[9] J. Goslin, M. Recq, and R. Schlich. Emplacement and evolution of the madagascar ridge and crozet submarine plateau. *Bull. Soc. Géol. Fr.*, 7:609–618, 1981.

[10] Chevallier L. Carte géologique au 1:50 000. archipel crozet, ile de la possession. *Comité Nation. Français Rech. Antarct.*, 50:16 pp., 1 map, 1981.

[11] L. Chevallier, J. Nougier, and J.M. Cantagrel. *Volcanology of Possession Island, Crozet Archipelago (TAAF)*, pages 652–658. Cambridge Univ, Cambridge Univ., 1983.

[12] E. Thellier and O. Thellier. Recherches géomagnétiques sur les coulées volcaniques d'auvergne. *Ann. Geophys.*, 1:37–52, 1944.

[13] M. Prévot. Some aspects of magnetic viscosity on subaerial and submarine volcanic rocks. *Geophys. J. R. Astr. Soc.*, 66:169–192, 1981.

[14] D.J. Dunlop. Viscous magnetization of 0.04-100 μm magnetites. *Geophys. J. Roy. Astron. Soc.*, 74:667–687, 1983.

[15] J. Edwards. Gyroremanent magnetization produced by specimen rotation between successive alternating field treatments. *Geophys. J. R. astr. Soc.*, 71:199–214, 1982.

[16] P. Roperch and G.K. Taylor. The importance of gyromagnetic remanence in alternating field demagnetization. some new data and experiments on g.r.m. and r.r.m. *Geophys. J. R. astr. Soc.*, 87:949–965, 1986.

[17] A. Stephenson. A gyroremanent magnetization in anisotropic magnetic material. *Nature*, 284:49, 1980.

[18] P.H. Dankers and J.D.A. Zijderveld. Alternating field demagnetization and the problem of gyro-magnetic remanence. *Earth Planet. Sci. Lett.*, 53:89–92, 1981.

[19] P. Camps and M. Prévot. A statistical model of the fluctuations in the geomagnetic field from paleosecular variation to reversal. *Sciences*, 273:776–779, 1996.

[20] J.L. Kirschvink. The least-squares line and plane and the analysis of paleomagnetic data. *Geophys. J. R. astr. Soc.*, 62:699–718, 1980.

[21] J. J. Love. Statistical assessment of preferred transitional VGP longitudes based on palaeomagnetic lava data. *Geophys. J. Int.*, 140(1):211–221, 2000.

[22] B. Efron and R. Tibshirani. Boostrap methods for standard errors, confidence intervals, and other measures of statistical accuracy. *Stat. Sci.*, 1:54–77, 1986.

[23] B.M. Gunn, E.C. Abranson, N.D. Watkins, and J. Nougier. *Petrology and geochemistry of Iles Crozet: a summary*, pages 825–829. Universitets forlaget Oslo, Oslo, 1972.

[24] C. Laj, A. Mazaud, R. Weeks, M. Fuller, and E. Herrero-Bervera. Geomagnetic reversal paths. *Nature*, 541:447, 1991.

[25] J.J. Love. Paleomagnetic volcanic data and geometric regularity of reversals and excursions. *J. Geophys. Res.*, 103(B6):12435–12452, 1998.

[26] P. Camps, R.S. Coe, and M. Prévot. Transitional geomagnetic impulse hypothesis : Geomagnetic fact or rock-magnetic artifact ? *J. Geophys. Res.*, 104(B8):17747–17758, 1999.

[27] M. Prévot and P. Camps. Absence of preferred longitude sectors for poles from volcanic records of geomagnetic reversals. *Nature*, 366:53–57, 1993.

[28] S.C. Cande and D.V. Kent. Revised calibration of the geomagnetic polarity timescale for the Late Cretaceous and Cenozoic. *J. Geophys. Res.*, 100:6093–6095, 1995.

Figure 1: Sketch showing locations of sampled sections on a geological map redrawn from [10].
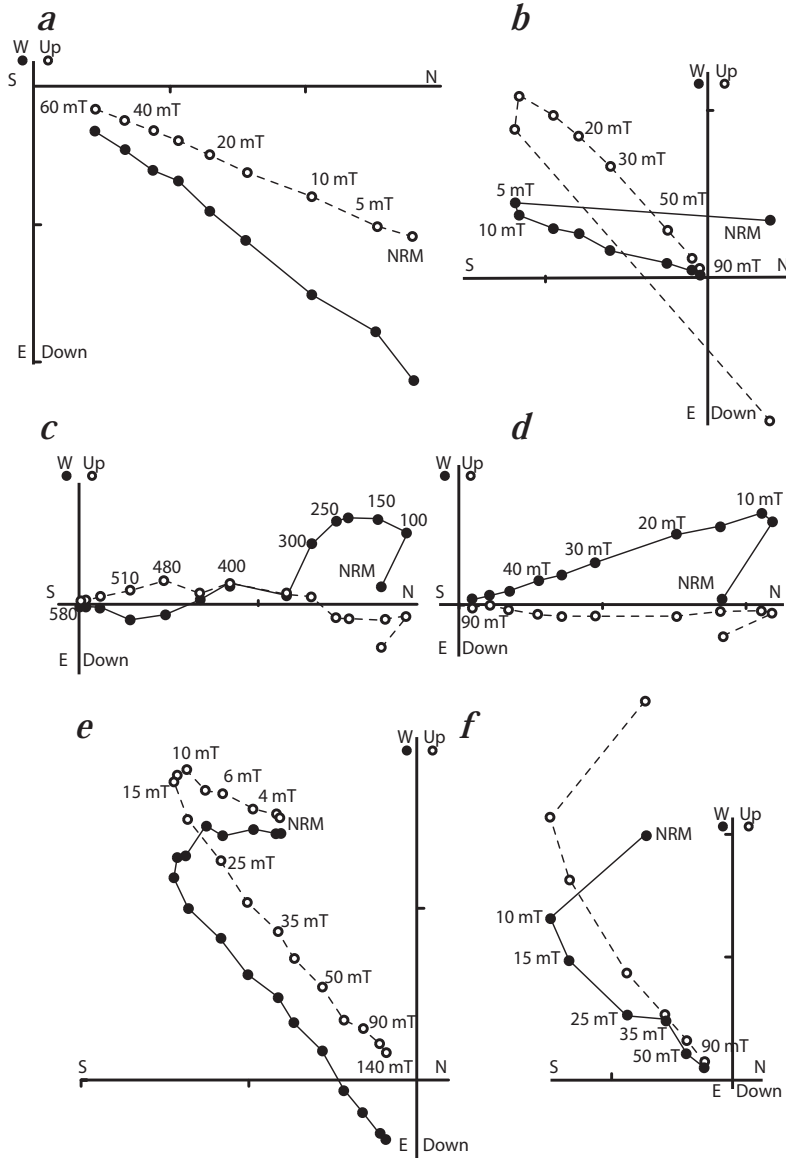
Figure 2: Orthogonal vector plots of stepwise paleomagnetic cleaning of representative samples (core coordinates). Example of samples with no significant overprint (a) flow AL14, specimen 193C, and strong viscous overprint (b) flow PC2, specimen 14C. Demagnetization diagrams of two specimens from the same core (flow CN15) illustrate the poor quality of thermal treatment of (c) specimen 310B compared to AF cleaning of (d) specimen 310A and the acquisition of spurious GRM component of (e) flow PC1, specimen 005A which is successfully removed (f) specimen 005C following a special procedure (see text for explanation).
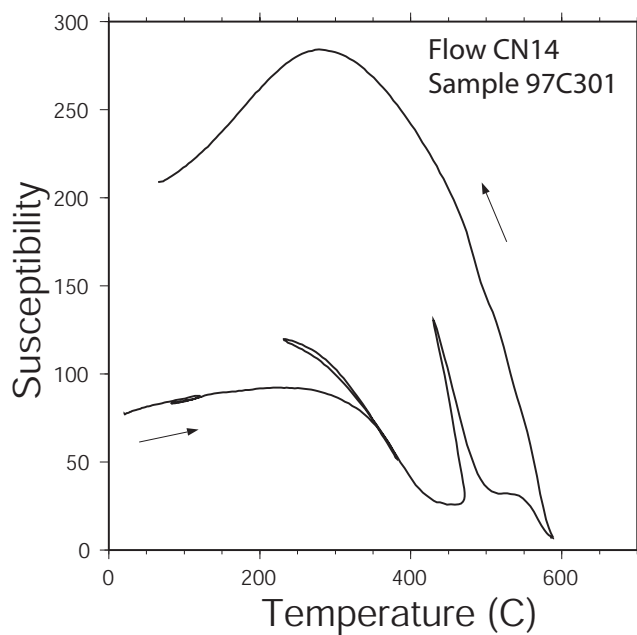
Figure 3: Example of thermal dependence of weak field magnetic susceptibility under vacuum. Heating and cooling curves are indicated by arrows. For the few samples measured, the curves are always irreversible.
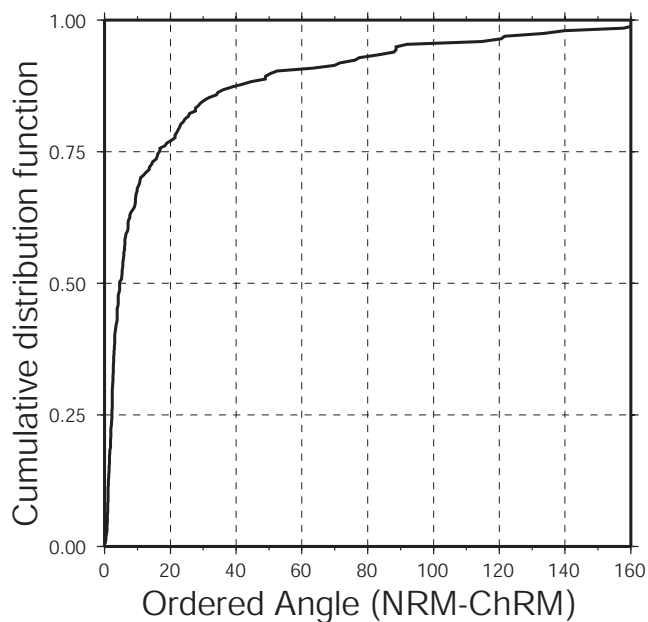
Figure 4: Cumulative distribution function for the angles between the ChRM and NRM directions.
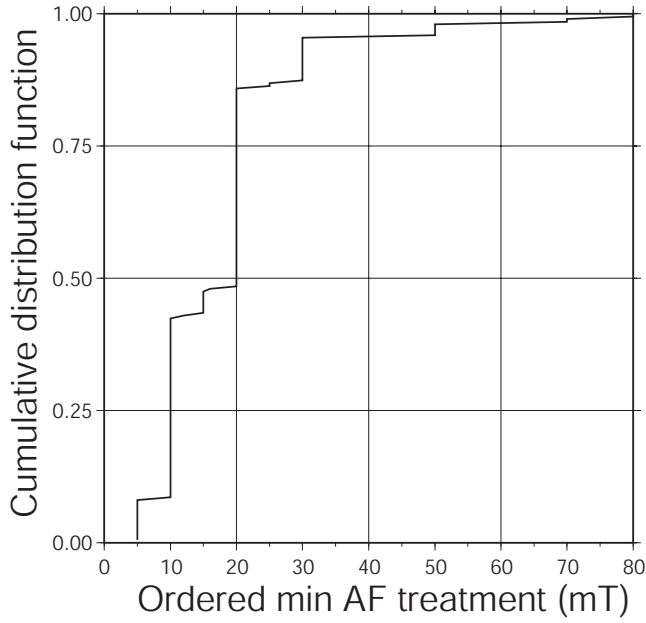
Figure 5: Cumulative distribution function of the first AF value used in the least squares analysis to compute the direction of ChRM.
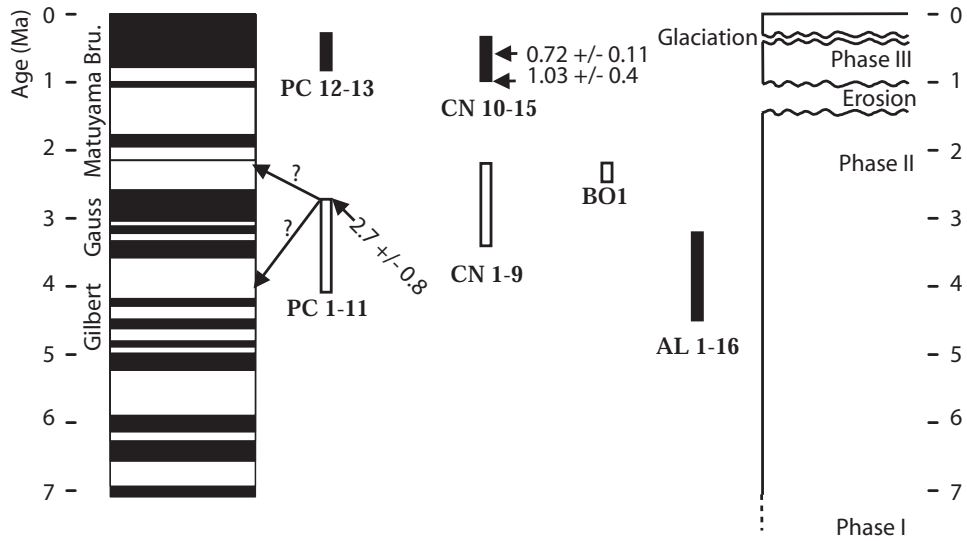
Figure 6: Relationship between the sampled sections, the geomagnetic polarity timescale for the last 7 Myr [28], and the chronostratigraphic evolution of Possession Island [11]. (See text for explanation.)

Figure 7: Virtual geomagnetic pole positions for Possession Island lava flows. Equal Area projection of a portion of (a) Northern and (b) Southern Hemisphere. Circles, AL section; solid triangles, PC section; open triangles, BO unit; squares, CN section.

14

Table 1: Directional Results

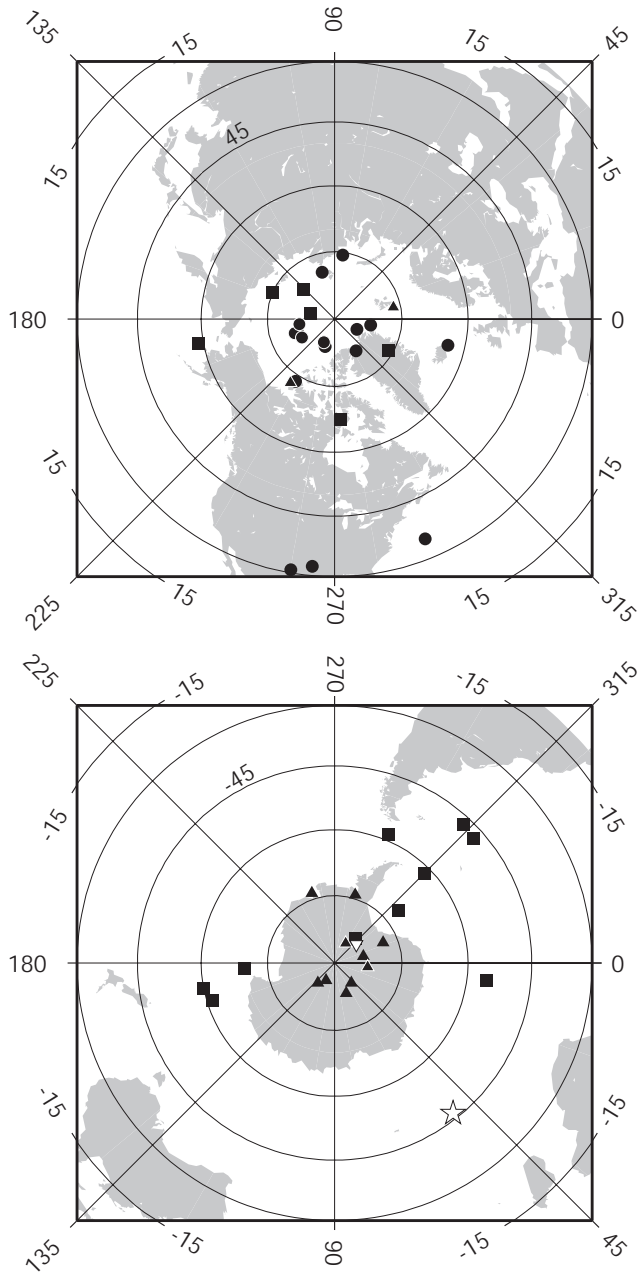| Flow	Phase	n/N	I	D	α_{95}	κ	Longitude	Latitude	J_0	J_{20}
Petit Caporal section (Latitude:-46.37°; Longitude:51.76°)										
pc13	III	7/7	-55.1	349.3	6.4	90	11.2	76.6	5.53	2.57
pc12	III	7/7	-76.1	357.6	3.7	269	235.3	72.7	5.86	2.91
pc11	II	7/7	50.0	186.5	3.3	330	251.9	-73.6	2.35	1.25
pc10	II	6/7	66.4	189.0	5.7	139	347.3	-83.4	2.63	0.87
pc9	II	8/8	68.8	180.3	2.4	528	49.9	-84.2	2.58	1.76
pc8	II	9/9	65.8	174.1	4.4	138	116.9	-85.7	2.75	1.00
pc7[b]	II	0/7							3.88	1.21
pc6	II	7/7	67.4	180.1	7.6	54	68.7	-82.8	1.25	0.80
pc5	II	7/7	65.2	171.6	4.3	198	129.9	-84.2	1.14	1.00
pc4	II	5/7	63.1	186.8	9.7	63	303.7	-84.9	1.37	0.86
pc3	II	5/5	65.9	197.1	8.0	92	336.9	-78.3	1.64	1.09
pc2	II	7/7	68.2	188.4	7.6	64	6.8	-82.6	1.85	0.60
pc1	II	5/7	55.5	196.1	16.0	24	286.9	-74.1	2.15	0.86
Alouette mountain section (Latitude:-46.38°; Longitude:51.78°)										
al16	II	8/8	-61.0	350.5	2.2	619	350.8	81.9	6.68	3.74
al15	II	7/7	-53.1	8.8	2.6	444	82.9	75.6	4.64	3.04
al14	II	7/7	-58.6	11.1	4.5	183	104.7	79.2	4.95	2.12
al13	II	8/8	-70.0	5.3	4.4	158	209.6	81.7	8.51	3.48
al12	II	7/7	-75.8	244.5	2.6	525	260.1	30.8	5.47	2.80
al11	II	8/8	-74.6	252.7	8.6	43	264.8	32.4	7.79	2.39
al10	II	4/4	-62.5	278.3	4.3	458	292.4	35.0	5.16	2.17
al9	II	7/7	-66.0	347.7	2.4	617	304.2	81.5	6.79	4.60
al8	II	10/10	-63.3	352.4	2.6	340	335.3	84.5	4.67	2.14
al7	II	6/7	-71.1	1.2	4.1	272	237.8	73.6	11.55	3.44
al6	II	7/7	-68.6	357.8	4.0	232	245.5	84.3	7.05	4.56
al5	II	12/12	-70.1	8.5	3.2	186	199.8	80.6	5.84	2.32
al4	II	2/3	-69.8	7.8			200.1	81.2	9.08	6.59
al3	II	7/7	-69.0	356.5	4.0	228	250.9	83.5	6.48	3.76
al2	II	7/7	-68.5	8.8	2.8	455	188.1	82.1	7.62	3.16
al1	II	7/7	-50.7	332.2	3.8	255	346.9	63.9	3.52	1.14
Bollard section (Latitude:-46.43°; Longitude:51.87°)										
bo1	II	7/8	63.4	189.0	4.6	130	311.9	-83.5	7.27	1.78
Crique de Noël section (Latitude:-46.46°; Longitude:51.83°)										
cn15	III	5/7	-74.0	329.4	7.1	79	273.2	67.5	3.10	2.56
cn14	III	6/7	-66.2	7.7	4.6	153	166.9	84.4	5.30	
cn13	III	3/4	-66.0	22.0	4.5	327	157.0	75.0	5.25	0.95
cn12	III	3/5	-75.4	47.8	5.1	254	190.3	58.9	9.06	3.27
cn11	III	6/7	-61.7	341.0	6.1	87	329.8	76.1	11.99	5.20
cn10	III	8/9	-63.2	13.5	9.1	29	136.2	80.4	7.05	1.72
cn9	II	7/8	74.7	234.8	6.5	66	7.7	-55.7	0.51	0.40
cn8	II	3/7	46.3	228.9	8.9	83	313.1	-47.5	2.68	2.90
cn7	II	5/7	45.5	210.1	6.5	91	292.9	-59.3	5.53	2.57
cn6	II	7/7	56.7	215.7	4.4	144	315.5	-62.2	5.14	2.26
cn5	II	7/7	50.1	231.0	4.3	150	318.6	-48.1	1.96	1.08
cn4	II	5/7	62.2	205.0	5.2	147	321.3	-72.1	2.73	1.71
cn3	II	7/8	50.5	147.6	2.7	379	161.8	-60.8	3.14	0.94
cn2	II	7/7	46.8	148.9	5.9	70	168.0	-59.5	2.00	0.96
cn1	II	7/7	52.7	159.6	3.7	287	174.9	-69.6	2.84	1.67

Flows are listed in stratigraphic order with the youngest on top, oldest on the bottom. The volcanic phases are inferred from the geological map (Figure 1) [10] and field observations; n/N is the number of samples used in the analysis/total number of samples collected; I and D are the mean inclination positive downward and declination east of north, respectively; α_{95} is 95% confidence cone about average direction; Longitude and Latitude correspond to VGP position; J_0 and J_{20} are the geometric mean remanence intensities in A/m of NRM and after 20 mT alternating field treatment, respectively.

Table 2: Dispersion Statistics of Flow-Average Directions

	VGP $> 45°$	VGP $> 55°$
N	41	39
Mean inclination	-64.4°	-64.7°
Mean declination	5.2°	1.9°
Precision parameter kappa	37.2	46.5
α_{95}	3.7°	3.4°
Mean of the within-flow asd S_W	5.6°	5.5°
Dispersion from the Dipole Field Direction ($I_m = -64.6$ $D_m = 0.0$)		
Total asd S_T	13.6° (13.0)	12.0° (11.6)
Between-flow asd S_B	13.4° (12.9)	11.8° (11.5)
95% confidence limits on S_B	10.4-16.2°	9.3-14.0°
Dispersion from the Mean Direction		
Total asd S'_T	13.4° (12.9)	12.0° (11.5)
Between flow asd S'_B	13.2° (12.7)	11.7° (11.3)
95% confidence limits on S'_B	10.4-15.9°	9.2-14.1°

N, number of lava flow included in the analysis; asd, angular standard deviation; see text for explanation of subscripts T, W, and B. The 95% confidence limits are computed using the jackknife method [22]. Numbers in parentheses correspond to asd calculated from [1] data set.

Table 3: Dispersion statistics of Virtual Geomagnetic Poles

	VGP $> 45°$	VGP $> 55°$
Possession Island		
N	41	39
Average VGP latitude	86.4°	88.0°
Average VGP longitude	157.3°	179.2°
Precision parameter Kappa	19.6	24.1
α_{95}	5.2°	4.8°
Total asd S_T	18.9° (17.2)	16.8° (15.5)
Mean of the within-flow asd S_W for VGP	7.8°	7.6°
Between-flow asd S_B	18.6°	16.5°
95% confidence limits on S_B	14.6-22.4°	13.2-19.6°
Marion Island, [7]		
N	21	20
Total asd S_T	20.3°	18.7°
Mean of the within-flow asd S_W for VGP	10.9°	11.0°
Between-flow asd S_B	19.9°	18.3°
95% confidence limits on S_B	14.8-24.2°	13.9-21.9°
Possession and Marion Combined		
N	62	59
Total asd S_T	19.2°	17.3°
Mean of the within-flow asd S_W for VGP	8.5°	8.4°
Between-flow asd S_B	18.9°	17.0°
95% confidence limits on S_B	15.9-21.7°	14.4-19.3°

N, number of lava flow included in the analysis; asd, angular standard deviation; see text for explanation of subscripts T, W, and B. The 95% confidence limits are computed using the jackknife method [22]. Numbers in parentheses correspond to asd calculated from [1] data set.